Protein-Resistant Silicones: Incorporation of Poly(ethylene oxide) via Siloxane Tethers

Ranjini Murthy,[†] Casey D. Cox,[†] Mariah S. Hahn,[‡] and Melissa A. Grunlan*[,†]

Departments of Biomedical Engineering and Chemical Engineering, Texas A&M University, College Station, Texas 77843-3120

Received May 17, 2007; Revised Manuscript Received July 3, 2007

Silicones with enhanced protein resistance were prepared by introducing poly(ethylene oxide) (PEO) chains via siloxane tethers **(a−c)** of varying lengths. Three unique ambifunctional molecules **(a−c)** having the general formula α-$(EtO)_3Si(CH_2)_2$-oligodimethylsiloxane$_n$-*block*-poly(ethylene oxide)$_8$-OCH_3 ($n = 0$ **(a)**, 4, **(b)**, and 13 **(c)**) were prepared via regioselective Rh-catalyzed hydrosilylation. Nine films were subsequently produced by the H_3PO_4-catalyzed sol−gel cross-linking of **a**−**c** each with α,ω-bis(Si−OH)polydimethylsiloxane (**P**, $M_n = 3000$ g/mol) in varying ratios (1:1, 1:2, and 2:3 molar ratio **a**, **b**, or **c** to **P**). Films prepared with a 2:3 molar ratio (**a**−**c** to **P**) contained the least amount of un-cross-linked materials, which may migrate to the film surface. For this set of films, surface hydrophilicity and protein resistance increased with siloxane tether length **(a−c)**. These results indicate that PEO was more effectively mobilized to the surface if incorporated into silicones via longer siloxane tethers.

Introduction

Silicones, particularly poly(dimethylsiloxane) (PDMS), have been utilized in many biomedical applications because of their thermal and oxidative stability, gas permeability, low modulus, flexibility, and good biocompatibility.[1,2] Unfortunately, silicones generally exhibit poor resistance to blood proteins as a result of its extreme hydrophobicity.[3,4] An adsorbed blood protein layer can invoke subsequent platelet adhesion and activation of coagulation pathways leading to thrombosis thereby compromising device success.[5,6] To reduce protein adsorption, silicone surfaces have been hydrophilized by various approaches that involve physical or chemical treatments or a combination of both.[3,7−10]

Poly(ethylene oxide) (PEO, or poly(ethylene glycol) (PEG)) is a neutral, hydrophilic polymer that exhibits unusually high protein resistance.[11,12] To improve the protein resistance of silicone surfaces, PEO has been incorporated into silicone materials. Typically, silyl methyl (Si−Me) groups at the surfaces of silicones are first converted to reactive silanol (Si−OH) groups by oxygen or air plasma,[13−15] UV radiation,[16,17] UV/ozone radiation (UVO),[16,18] or solution-phase oxidation.[19] PEO may be subsequently grafted onto the silanol-covered silicone surfaces via silanization reactions of PEO−silanes containing appropriate end-functionalized silane anchoring groups such as alkoxysilanes.[20] For instance, both trimethoxysilylpropyl and triethoxysilylpropyl PEO monomethyl ether ($(RO)_3Si(CH_2)_3-(OCH_2CH_2)_n-OCH_3$) have been effectively grafted onto silanol-covered silicone surfaces.[19,21,22] Silane (Si−H)-enriched silicone surfaces, produced by acid-catalyzed equilibration of silicone in the presence of polymethylhydrosiloxane, were grafted with allyl PEO monomethyl ether ($CH_2{=}CHCH_2-(OCH_2CH_2)_n-OCH_3$) via Pt-catalyzed hydrosilylation.[23] PEO has also been introduced throughout the bulk of silicone materials via the condensation cure of triethoxysilylpropyl PEO monomethyl ether with α,ω-bis(Si−OH)PDMS and tetraethoxysilane ($Si(OEt)_4$).[24,25]

PEO's protein resistance has been attributed to its high water content,[26] large excluded volume,[27] steric repulsion,[28,29] and its blockage of adsorption sites on the underlying surface.[30] The effect of PEO molecular weight (MW) and surface concentration on protein resistance has been widely studied.[11,31−37] The configurational mobility of PEO produces an entropic penalty of chain compression if protein adsorption were to occur.[12,28,29] Thus, enhancement of PEO chain mobility may optimize protein resistance. For instance, surfaces of coatings prepared by cross-linking α,ω-bis(Si−OH)PDMS with *bis*-triethoxysilylpropyl PEO displayed inferior protein resistance compared to surfaces of coatings prepared with triethoxysilylpropyl PEO monomethyl ether.[25] This was attributed to a lack of mobilization of the difunctional PEO to the aqueous interface compared to the monofunctional PEO. Conventional strategies to incorporate PEO into silicones utilize PEO−silanes in which the PEO segment is separated from the grafting or cross-linking site by a short alkane spacer (e.g., propyl as for $(RO)_3Si(CH_2)_3-(CH_2-CH_2O)_n-OCH_3$)), which may limit PEO mobility.[19,21−25]

Herein, we propose a synthetic strategy to prepare silicones with enhanced protein resistance by the incorporation of PEO via siloxane tethers. Three unique ambifunctional molecules **(a−c)** were prepared having the general formula α-$(EtO)_3Si(CH_2)_2-$oligodimethylsiloxane$_n$-*block*-poly(ethylene oxide)$_8-OCH_3$ ($n = 0$ **(a)**, 4, **(b)**, and 13 **(c)**) (Figure 1). Thus, the PEO segment is distanced from the cross-linkable group ($(EtO)_3Si$) by an oligodimethylsiloxane tether. These siloxane tethers are highly flexible due to the wide bond angle (~143°) and low barrier to linearization (0.3 kcal/mol) of Si−O−Si of dimethylsiloxanes.[38,39] The dynamic flexibility of Si−O−Si produces polymers with extremely low glass transition temperatures (T_g's) (e.g., PDMS, $T_g = -125$ °C). Thus, the siloxane tethers of **a**−**c** should enhance PEO chain mobility so that PEO is more effectively reorganized to film surfaces to improve protein resistance.

* Author to whom correspondence should be addressed. E-mail: mgrunlan@tamu.edu.
[†] Department of Biomedical Engineering.
[‡] Department of Chemical Engineering.

10.1021/bm700543c CCC: $37.00
Published on Web 08/29/2007

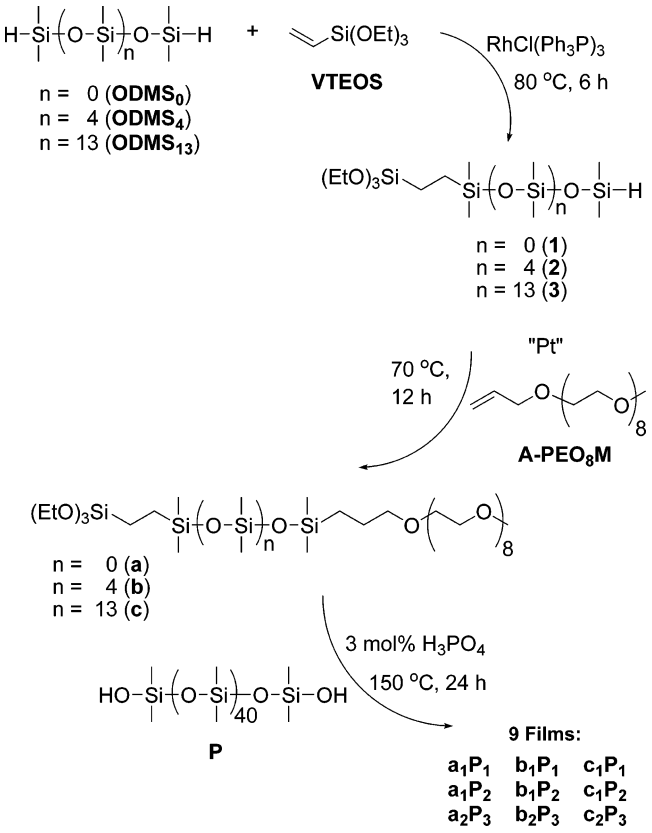

Figure 1. Synthesis of **a**−**c** and subsequent conversion to cross-linked films by the acid-catalyzed sol−gel condensation with α,ω-bis(Si−OH)polydimethylsiloxane (**P**) at 1:1, 1:2, and 2:3 molar ratios of **a**, **b**, or **c** to **P**.

To prepare ambifunctional molecules **(a**−**c)**, we utilized regioselective hydrosilylation reported by Crivello and Bi.[40−43] Rhodium-catatalyzed (Wilkinson's catalyst, $RhCl(Ph_3P)_3$) hydrosilylation of α,ω-bis(Si−H)oligodimethylsiloxanes with vinyl-terminated molecules was shown to proceed in a regioselective fashion. Thus, only one of the two terminal Si−H moieties was added to the vinyl compound. In this study, a series of three commercially available α,ω-bis(Si−H)oligodimethylsiloxanes$_n$ (**ODMS$_0$**, **ODMS$_4$**, and **ODMS$_{13}$**) were utilized. Alternatively, **ODMS$_4$** and **ODMS$_{13}$** may be prepared by the acid-catalyzed equilibration of cyclic siloxanes such as octamethylcyclotetrasilaxane (D_4) or hexamethyltrisiloxane (D_3) with tetramethyldisiloxane (TMDS) by varying the stoichiometry of the cyclic siloxanes and TMDS.[44,45] A cross-linkable $(EtO)_3Si$− moiety was introduced to one terminal end of each α,ω-bis(Si−H)oligodimethylsiloxane (**ODMS$_{0,4,13}$**) by regioselective Rh-catalyzed hydrosilylation with vinyl triethoxysilane (**VTEOS**) to yield the corresponding α-triethoxysilylethyl-ω-silane-oligodimethylsiloxane$_n$ (**1**−**3**) (Figure 1). The Pt-catalyzed (Karstedt's) hydrosilylation reaction of the regioselective products (**1**−**3**) each with allyl PEO monomethyl ether (M_n = 425 g/mol) yielded the corresponding ambifunctional molecules **(a**−**c)**. Although we obtained the allyl PEO monomethyl ether from a commercial source, it may be prepared by reaction of monomethoxy PEO with NaH and allyl bromide.[46] Finally, **a**−**c** each underwent phosphoric acid (H_3PO_4)-catalyzed sol−gel cross-linking with α,ω-bis(Si−OH)polydimethylsiloxane (**P**, M_n = 3000 g/mol) in varying ratios (1:1, 1:2, and 2:3 molar ratios of **a**, **b**, or **c** to **P**) to produce nine compositional unique films.[47]

Experimental Section

Polymer Characterization. *NMR.* ^1H and ^{13}C spectra were obtained on a Mercury 300 MHz spectrometer operating in the Fourier transform mode. Five percent (w/v) $CDCl_3$ solutions were used to obtain spectra. ^{13}C NMR spectra were run with broad-band proton decoupling. Residual $CDCl_3$ was used as an internal standard.

IR Spectroscopy. IR spectra of neat liquids on NaCl plates were recorded using a Bruker TENSOR 27 Fourier transform infrared spectrometer.

Gel Permeation Chromatography. Gel permeation chromatography (GPC) analysis was performed on a Viscotek GPC system equipped with three detectors in series: refractive index (RI), right angle laser light scattering (RALLS), and viscometer (VP). The ViscoGEL HR-Series (7.8 mm × 30 cm) column packed with divinylbenzene cross-linked polystyrene was maintained at 25 °C in a column oven. The eluting solvent was HPLC grade toluene at a flow rate of 1.0 mL/min. The detectors were calibrated with a polystyrene narrow standard with the following parameters: M_w (66 000 g/mol), polydispersity (1.03), intrinsic viscosity (0.845 dL/g), and d*n*/d*c* (0.112 mL/g). Data analysis was performed with Viscotek OmniSec software (version 4.0).

Thermal Gravimetric Analysis. The thermal stabilities of neat liquid samples (∼10 mg) in Pt pans were evaluated with a TA Instruments Q50 under N_2 or air at a flow rate of 40 cm^3/min. The sample weight was recorded while the temperature was increased 4 °C/min from 25 to 800 °C.

Film Characterization. *Thermal Gravimetric Analysis.* Thermal analyses of free-standing pieces of films (∼10 mg) were similarly measured as described above.

Soxhlet Extraction. The amount of un-cross-linked material in a film was determined by Soxhlet extraction. A film cured on a microscope slide was extracted with CH_2Cl_2 in a Soxhlet apparatus for 12 h. The percentage of un-cross-linked material was calculated as the weight difference of the extracted versus unextracted weight divided by the unextracted weight.

Dynamic Mechanical Analysis. Storage (G') and loss (G'') moduli of cured films were measured as a function of temperature on a TA Instruments Q800 dynamic mechanical analyzer. Specimens (length × width = 35 × 5.3 mm^2) were cut from free-standing films using a clean single-edged razor cutting tool. Electronic calipers were used to measure film thickness (∼0.5 mm) prior to testing. The dynamic mechanical analyzer was operated using a dual cantilever clamp assembly at a frequency of 5 Hz and a displacement of 4 μm. After equilibration at −140 °C for 3 min, the temperature was increased 4 °C/min to 25 °C. The T_g was determined from the peak maximum of the measured G''.

Contact Angle Measurement. Static (θ_{static}), advancing (θ_{adv}), and receding (θ_{rec}) contact angles of distilled/deionized water droplets at the film−air interface were measured at room temperature (RT) with a CAM-200 (KSV Instruments) contact angle measurement system equipped with an autodispenser, video camera, and drop-shape analysis software. Coated microscope slides were stored in a desiccator for 5 days prior to contact angle measurements. For θ_{static} measurements, a sessile drop of water (5 μL) was measured at 15 s and 2 min after deposition onto the film surface. The θ_{adv} was measured by the addition of 3 μL (0.25 μL/s) of water to a 5 μL pendant droplet to advance the contact line. The θ_{rec} was measured by the subsequent removal of 4 μL (0.25 μL/s) from the same droplet to recede the contact line. The reported θ_{static}, θ_{adv}, and θ_{rec} values are an average of three measurements taken on different areas of the same film sample.

Adsorption of Bovine Serum Albumin Protein. The adhesion of Alexa Fluor 555 dye conjugate of bovine serum albumin (AF-555 BSA; M_w = 66 kDa; Molecular Probes, Inc.) onto film surfaces was studied by fluorescence microscopy. To remove residual acid catalyst from the films, all coated microscope slides were first leached in distilled water for 24 h with fresh water changes every 6 h until the pH of the water remained at ∼7.2. Coated microscope slides were subsequently dried in vacuo (36 in. Hg, 24 h, RT) and stored in a desiccator for 2 days

prior to testing. A silicone isolator (20 mm well diameter, 2.5 mm well depth; JTR Press-to-Seal Silicone Isolators) was affixed to each coated microscope slide with clips to prevent leakage of solutions from the well. For each film composition, two coated microscopes slides were analyzed. One slide served to test a film surface exposed to air prior to AF-555 BSA deposition whereas the other served to test a film surface that was first exposed to phosphate-buffered saline (PBS; pH = 7.4) for 12 h.

For air-equilibrated films, the exposed surface of the film inside each isolator well was filled with 1 mL of AF-555 BSA solution (0.1 mg/mL in PBS), equilibrated in the dark at RT for 3 h, and removed. One milliliter of fresh PBS was then added to each well and removed after 5 min; this process was repeated a total of three times. Film surfaces tested in this way are referred to as "air-equilibrated".

For PBS-equilibrated films, on the second set of coated microscope slides, the exposed surface of the film inside each isolator was filled with 1 mL of PBS and removed after 12 h. Exposure to AF-555 BSA solution (3 h) was immediately executed using the same protocol as above. Film surfaces tested in this manner are referred to as "PBS-equilibrated".

A Zeiss Axiovert 200 optical microscope equipped with a A-Plan 5× objective (Axiocam HRC revision 2) and filter cube (excitation filter of 546 ± 12 nm (band-pass) and emission filter 575−640 nm (band-pass)) was used to obtain fluorescent images on three randomly selected regions of the surface within each isolator well. The fluorescent light source was permitted to warm up for 30 min prior to image capture. Linear operation of the camera was ensured, and the constant exposure time used during the image collection permitted quantitative analyses of the observed fluorescent signals. The fluorescence microscopy images were analyzed using the histogram function of Photoshop, which yielded the mean and standard deviation of the fluorescence intensity within a given image. The fluorescence intensity of each AF-555-BSA-exposed region was subtracted from that of nonexposed region to ensure correction for any fluorescence signal from the material itself. The background-corrected fluorescence intensities for each film were then used to quantify AF-555 BSA levels adsorbed by comparison against a calibration curve constructed from the measured fluorescence intensities of AF-555 BSA standard slides. Standard slides were prepared by fitting a silicone isolator to uncoated, solvent-cleaned glass slides and adding 1 mL of AF-555 BSA solutions of known concentrations (0, 0.005, 0.01, 0.02, and 0.04 mg/mL AF-555 BSA in PBS) to individual wells.

X-ray Photoelectron Spectroscopy. X-ray photoelectron spectroscopy (XPS) was used to confirm the chemical grafting of $(EtO)_3Si-(CH_2)_3-(OCH_2CH_2)_8-OCH_3$ onto glass microscope slides, which served as the "PEO control". The surface was analyzed using a KRATOS AXIS Ultra Imaging X-ray photoelectron spectrometer with a Mg Kα nonmonochromatic X-ray source. The spot size was 7 mm × 3 mm. The survey scan (0−1100 eV) and C 1s high-resolution scan (20 eV scan width) were performed with a takeoff angle of 90°. Binding energies were referenced to the C−C peak at 285 eV. The raw data were analyzed using XPS peak processing software.

Materials. $RhCl(Ph_3P)_3$ (Wilkinson's catalyst) and solvents were obtained from Aldrich. HPLC grade toluene and NMR grade $CDCl_3$ were dried over 4 Å molecular sieves. Silastic T-2 (silicone elastomer) was obtained from Dow Corning. Pt−divinyltetramethyldisiloxane complex (Karstedt's catalyst), triethoxysilane, vinyltriethoxysilane (**VTEOS**), α,ω-bis(Si−H)oligodimethylsiloxanes (**ODMS$_0$** or tetramethyldisiloxane; **ODMS$_4$**, M_n = 400−500 g/mol per manufacturer's specifications; **ODMS$_{13}$**, M_n = 1000−1100 g/mol per manufacturer's specifications), α,ω-bis-(Si−OH)polydimethylsiloxane (**P,** M_n = 2000−3500 g/mol per manufacturer's specifications), and monovinyl-terminated PDMS (**CH_2=CH−PDMS-*n*-Bu**, M_n = 62 700 g/mol, essentially 100% monovinyl-terminated with the nonfunctional end *n*-butyl-terminated per manufacturer's specifications) were acquired from Gelest. The number average molecular weight (M_n) of **ODMS$_0$**, **ODMS$_4$**, and **ODMS$_{13}$** were determined by ^{1}H NMR end-group analysis: **ODMS$_0$** (134 g/mol), **ODMS$_4$** (430 g/mol), and **ODMS$_{13}$** (1096 g/mol). The MWs of **P** were determined by GPC (M_w/M_n = 5000/3000 g/mol). PEO allyl methyl ether (**A-PEO$_8$M**) was obtained from Clariant (Polyglykol AM-500) and was dried overnight under high vacuum prior to use. The M_n of **A-PEO$_8$M** was determined to be 425 g/mol (n = 8) by end-group analysis. ^{1}H NMR (δ, ppm): 3.26 (s, 3H, OCH_3), 3.51 (m, 32H, OCH_2CH_2), 3.90 (d, 2H, J = 5.7 Hz, CH_2=$CHCH_2O$), 5.11 (m, 2H, CH_2=$CHCH_2O$), and 5.79 (m, 1H, CH_2=$CHCH_2O$).

Table 1. Film Compositions and Percentage Weight Loss after Soxhlet Extraction

film	**a**, **b**, or **c** (value of *n*)	moles of **a**, **b**, or **c**	moles of **P** (HOSi−PDMS$_{40}$−SiOH)	% wt loss[a]
a_1P_1	**a** (n = 0)	1	1	1%
b_1P_1	**b** (n = 4)	1	1	3%
c_1P_1	**c** (n = 13)	1	1	2%
a_1P_2	**a** (n = 0)	1	2	9%
b_1P_2	**b** (n = 4)	1	2	8%
c_1P_2	**c** (n = 13)	1	2	4%
a_2P_3	**a** (n = 0)	2	3	0.5%
b_2P_3	**b** (n = 4)	2	3	1%
c_2P_3	**c** (n = 13)	2	3	0.5%

[a] After Soxhlet extraction (CH_2CH_2, 12 h), corresponds to percentage of un-cross-linked material: 1:1 molar ratio **a**−**c** to **P**, stoichiometric excess of **a**−**c**; 1:2 molar ratio **a**−**c** to **P**, stoichiometric excess of **P**; 2:3 molar ratio **a**−**c** to **P**, stoichiometric balance.

Synthetic Approach. All reactions were run under a N_2 atmosphere with a Teflon-covered stir bar to agitate the reaction mixture.

α-Triethoxysilylethyl-ω-silane-oligodimethylsiloxanes$_n$ (**1**−**3**) were prepared by the Rh-catalyzed regioselective hydrosilylation of equimolar amounts of **VTEOS** with **ODMS$_0$**, **ODMS$_4$**, or **ODMS$_{13}$**, respectively (Figure 1). **ODMS$_n$** and **VTEOS** (1:1 molar ratio) were combined with Wilkinson's catalyst and toluene into a 350 mL pressure vessel equipped with a Teflon bushing as a pressure seal. The tube was sealed and heated to 80 °C. After 6 h, the reaction was cooled to room temperature, and toluene was removed under reduced pressure. The residue was purified by flash column chromatography on silica gel with hexanes/ethyl acetate (2:1 v/v), and volatiles were removed under reduced pressure.

Triethoxysilylethyl-oligodimethylsiloxane$_n$-*block*-poly(ethylene oxide)$_8$ (**a**−**c**) were prepared by the Pt-catalyzed hydrosilylation of **A-PEO$_8$M** with **1**, **2**, or **3**, respectively (Figure 1). Polymers **1**−**3** were each combined with **A-PEO$_8$M** (1:1 molar ratio) and toluene in a round-bottom flask equipped with a rubber septum and heated to 70 °C. The progress of the reaction was monitored with IR spectroscopy by the disappearance of the Si−H (∼2125 cm^{-1}) absorbance. After an initial reaction time of ∼12 h, an aliquot of the reaction solution was evaporated on a NaCl plate, and the IR spectrum was obtained. In the case of an incomplete reaction, additional Karstedt's catalyst (50% of original volume) was added, and the reaction continued for another ∼6 h before checking the IR spectrum. This cycle was repeated until no Si−H absorbance was observed in the IR spectrum. Typically, no additional Kartstedt's catalyst was required to complete the reaction. The catalyst was removed from the reaction mixture by refluxing the reaction mixture with activated charcoal for 12 h. After filtration, the volatiles were removed under reduced pressure so that **a**−**c** were isolated as colorless liquids.

Film Preparation. In a scintillation vial equipped with a Teflon-covered stir bar and cap, **a**−**c** were each combined with α,ω-bis(Si−OH)polydimethylsiloxane (**P**, M_n = 3000 g/mol) in varying molar ratios (1:1, 1:2, and 2:3 molar ratios of **a**, **b**, or **c** to **P**) and mixed for ∼5 min (Table 1). Next, 3 mol % of H_3PO_4 (based on total solid weight of the aforementioned mixtures) was added as a solution of H_3PO_4/EtOH (10:90 w/w), and the mixture was stirred rapidly for 3 h.

Microscope slides (75 × 25 × 1 mm^3) were sequentially washed with distilled water, CH_2Cl_2/hexane (1:1 v/v), and acetone and finally

dried in a 150 °C oven for 24 h prior to use. One milliliter of each of the aforementioned mixtures was applied to a microscope slide and allowed to coat the entire slide. The slide was then placed in a level 150 °C oven for 24 h. Free-standing films for dynamic mechanical analysis (DMA) and thermal gravimetric analysis (TGA) testing were obtained by removing films from slides with a clean single-edge razor blade. Coated microscope slides were used for contact angle measurements and protein adsorption studies.

Triethoxysilylpropyl PEO monomethyl ether ($(EtO)_3Si-(CH_2)_3-(OCH_2CH_2)_8-OCH_3$) was chemically grafted onto microscope slides with typical procedures.[48] Briefly, clean microscope slides were immersed in HCl (12 M)/MeOH (1:1 v/v) for 2 h and then in HCl (12 M) for 2 h. The slides were rinsed thoroughly with deionized water and dried under vacuum at 50 °C for 4 h. The glass slides were then immersed in a solution of $(EtO)_3Si-(CH_2)_3-(OCH_2CH_2)_8-OCH_3$/toluene (5:95 v/v) for 12 h at RT. The slides were removed from the solution and cured at 180 °C in vacuo (36 in. Hg) for 12 h. PEO-grafted microscope slides served as the "PEO control" for contact angle and protein adsorption studies.

Silastic T-2 (silicone elastomer) was applied to clean microscope slides with a drawdown bar (30 mil) and allowed to cure at RT for over 72 h. The film thickness for cured Silastic T-2 films was ~0.6 mm. A silicone-coated slide served as a "PDMS control" for contact angle and protein adsorption studies.

Synthesis of 1. $ODMS_0$ (20.0 g, 0.15 mol), **VTEOS** (28.4 g, 0.15 mol), and Wilkinson's catalyst (10 mg) in toluene (100 mL) were reacted as above. In this way, **1** (43.4 g, 89% yield) was obtained. ^{1}H NMR (δ, ppm): 0.001−0.02 (m, 6H, $SiCH_3$), 0.06−0.12 (m, 6H, $SiCH_3$), 0.50 (m, 3H, $SiCH_2CH_2$), 1.03 (m, 1H, $SiCH_2CH_2$), 1.18 (m, 9H, $SiOCH_2CH_3$), 3.77 (m, 6H, $SiOCH_2CH_3$), 4.64 (m, 1H, Si*H*). ^{13}C NMR (δ, ppm): −0.44, 1.17, 2.03, 9.30, 9.50, 18.60, 58.62. IR (ν): 2125 (Si−H) cm^{-1}.

Synthesis of 2. $ODMS_4$ (20.05 g, 0.05 mol), **VTEOS** (8.46 g, 0.05 mol), and Wilkinson's catalyst (10 mg) in toluene (60 mL) were reacted as above. In this way, **2** (28.0 g, 90% yield) was obtained. ^{1}H NMR (δ, ppm): 0.001−0.15 (m, 36H, $SiCH_3$), 0.52 (m, 3H, $SiCH_2CH_2$), 1.04 (m, 1H, $SiCH_2CH_2$), 1.18 (m, 9H, $SiOCH_2CH_3$), 3.77 (m, 6H, $SiOCH_2CH_3$), 4.66 (m, 1H, Si*H*). ^{13}C NMR (δ, ppm): −0.25, 1.02, 1.19, 1.36, 1.51, 2.13, 9.45, 18.67, 58.70. IR (ν): 2125 (Si−H) cm^{-1}.

Synthesis of 3. $ODMS_{13}$ (20.1 g, 0.02 mol), **VTEOS** (3.5 g, 0.02 mol), and Wilkinson's catalyst (10 mg) in toluene (50 mL) were reacted as above. In this way, **3** (23.2 g, 90% yield) was obtained. ^{1}H NMR (δ, ppm): 0.001−0.17 (m, 78H, $SiCH_3$), 0.53 (m, 3H, $SiCH_2CH_2$), 1.05 (m, 1H, $SiCH_2CH_2$), 1.19 (m, 9H, $SiOCH_2CH_3$), 3.78 (m, 6H, $SiOCH_2CH_3$), 4.68 (m, 1H, Si*H*). ^{13}C NMR (δ, ppm): −0.31, 0.97, 1.13, 1.33, 1.45, 2.08, 9.40, 18.61, 58.67. IR (ν): 2125 (Si−H) cm^{-1}.

Synthesis of a. Polymer **1** (5.1 g, 0.016 mmol), **A-PEO_8M** (6.7 g, 0.016 mol), and Karstedt's catalyst (50 μL) in toluene (60 mL) were reacted as above. In this way, **a** (10.6 g, 88% yield) was obtained. ^{1}H NMR (δ, ppm): −0.07 to −0.06 (m, 12H, $SiCH_3$), 0.002 (m, 2H, $SiCH_2CH_2CH_2$), 0.43 (m, 3H, $SiCH_2CH_2$), 0.96 (m, 1H, $SiCH_2CH_2$), 1.12 (m, 9H, $SiOCH_2CH_3$), 1.47 (m, 2H, $SiCH_2CH_2CH_2$), 3.27 (s, 3H, OCH_3), 3.44 (m, 2H, $SiCH_2CH_2CH_2$), 3.54 (m, 32H, OCH_2CH_2), 3.71 (m, 6H, $SiOCH_2CH_3$). ^{13}C NMR (δ, ppm): −0.39, 0.29, 1.81, 9.21, 14.24, 18.33, 23.44, 58.31, 58.99, 70.03, 70.53−70.63, 71.95, 74.21. IR (ν): no Si−H band.

Synthesis of b. Polymer **2** (5.24 g, 0.008 mol), **A-PEO_8M** (3.48 g, 0.008 mmol), and Karstedt's catalyst (50 μL) in dry toluene (45 mL) were reacted as above. In this way, **b** (7.8 g, 91% yield) was obtained. ^{1}H NMR (δ, ppm): −0.02 to 0.01 (m, 36H, $SiCH_3$), 0.07 (m, 2H, $SiCH_2CH_2CH_2$), 0.50 (m, 3H, $SiCH_2CH_2$), 1.03 (m, 1H, $SiCH_2CH_2$), 1.16 (m, 9H, $SiOCH_2CH_3$), 1.53 (m, 2H, $SiCH_2CH_2CH_2$), 3.32 (s, 3H, OCH_3), 3.47 (m, 2H, $SiCH_2CH_2CH_2$), 3.56 (m, 32H, OCH_2CH_2), 3.73 (m, 6H, $SiOCH_2CH_3$). ^{13}C NMR (δ, ppm): −0.48, 0.21, 1.17, 1.28, 1.87, 9.19, 14.19, 18.43, 23.46, 58.45, 59.13, 70.12, 70.64−70.73, 72.05, 74.33. IR (ν): no Si−H band.

Synthesis of c. Polymer **3** (10.37, 0.008 mol), **A-PEO_8M** (3.42, 0.008 mol), and Karstedt's catalyst (50 μL) in toluene (50 mL) were reacted as above. In this way, **c** (12.1 g, 88% yield) was obtained. ^{1}H NMR (δ, ppm): −0.002 to 0.05 (m, 90H, $SiCH_3$), 0.09 (m, 2H, $SiCH_2CH_2CH_2$), 0.51 (m, 3H, $SiCH_2CH_2$), 1.05 (m, 1H, $SiCH_2CH_2$), 1.18 (m, 9H, $SiOCH_2CH_3$), 1.55 (m, 2H, $SiCH_2CH_2CH_2$), 3.34 (s, 3H, OCH_3), 3.52 (m, 2H, $SiCH_2CH_2CH_2$), 3.60 (m, 32H, OCH_2CH_2), 3.78 (m, 6H, $SiOCH_2CH_3$). ^{13}C NMR (δ, ppm): −0.45, 0.25, 1.21, 1.31, 1.92, 9.24, 14.24, 18.47, 23.51, 58.49, 59.16, 70.17, 70.69−70.79, 72.10, 74.38. IR (ν): no Si−H band.

Synthesis of $(EtO)_3Si-(CH_2)_3-(CH_2CH_2O)_8-OCH_3$. Triethoxysilane (3.07 g, 0.019 mol), **A-PEO_8M** (7.94 g, 0.019 mol), and Karstedt's catalyst (50 μL) in toluene (25 mL) were reacted as above to produce triethoxysilylpropyl PEO monomethyl ether $(EtO)_3Si-(CH_2)_3-(OCH_2CH_2)_8-OCH_3$ (9.3 g, 83% yield).[24] ^{1}H NMR (δ, ppm): 0.59 (m, 2H, $SiCH_2CH_2CH_2$), 1.18 (m, 9H, $SiOCH_2CH_3$), 1.61 (m, 2H, $SiCH_2CH_2CH_2$), 3.34 (m, 3H, OCH_3), 3.40 (m, 2H, $SiCH_2CH_2CH_2$), 3.61 (m, 32H, OCH_2CH_2), 3.78 (m, 6H, $SiOCH_2CH_3$). IR (ν): no Si−H band.

Discussion

Synthesis of 1−3. Rhodium-catalyzed regioselective hydrosilylation reaction of equimolar amounts of **VTEOS** with **$ODMS_0$**, **$ODMS_4$**, or **$ODMS_{13}$** effectively produced **1−3**, respectively, in good yields (≥89%) (Figure 1). ^{1}H NMR spectra of **1−3** showed a reduction in the Si−H peak integration value by one-half compared to the starting material. A Si−H (~2125 cm^{-1}) absorbance was noted in the IR spectra of **1−3**.

Verification of the Composition of 1−3. For Rh-catalyzed regioselective hydrosilylation, the enhanced reactivity of one Si−H terminus of α,ω-bis(Si−H)-terminated compounds toward vinyl-containing compounds is not well understood. However, the requirement for terminal Si−H groups within an appropriate distance has been suggested. For instance, the rate of regioselective hydrosilylation of bis(dimethylsilyl)alkanes is significantly reduced when the number of methylene units between Si−H groups is increased from 2 to 4.[49] Crivello and Bi reported the regioselective hydrosilylation of α,ω-bis(Si−H)oligodimethylsiloxanes having only 2−4 silicon atoms.[40−43] In this study, we utilized α,ω-bis(Si−H)oligodimethylsiloxanes (**$ODMS_0$**, **$ODMS_4$**, and **$ODMS_{13}$**) having 2, 6, and 15 silicon atoms, respectively. Evidence that **1−3** are the pure monosubstituted products of regioselective hydrosilylation cannot be solely based on ^{1}H NMR analysis because each spectrum represents the average composition of the sample. In other words, a pure monosubstituted product (**1**, **2**, or **3**) would have the same ^{1}H NMR spectrum as the mixture of three products obtained from the corresponding non-regioselective hydrosilylation, **(i)** α-triethoxysilylethyl-monosubstituted product (**1**, **2**, or **3**), **(ii)** α,ω-triethoxysilylethyl-disubstituted product, and **(iii)** nonsubstituted product (**$ODMS_0$**, **$ODMS_4$**, or **$ODMS_{13}$**), where the ratio of disubstituted to nonsubstituted product would be equal (Figure S2 of the Supporting Information). Because **$ODMS_{13}$** is the highest MW α,ω-bis(Si−H)oligodimethylsiloxane of the series, it is anticipated to be most likely to undergo non-regioselective Rh-catalyzed hydrosilylation. Thus, we sought to confirm that **3** was the pure monosubstituted product of regioselective hydrosilylation of **$ODMS_{13}$** and **VTEOS**.

Following Rh-catalyzed hydrosilylation of **$ODMS_{13}$** and **VTEOS** (1:1 molar ratio), the product was reacted with **CH_2═CH−PDMS-*n*-Bu** (M_w/M_n = 83 000/60 000 g/mol) by Pt-catalyzed hydrosilylation such that all Si−H groups were consumed (confirmed by IR) thereby producing **M**. Identifying whether or not **M** was the product of exclusively **3** + **CH_2═CH−PDMS-*n*-Bu** was then determined by GPC. If the initial

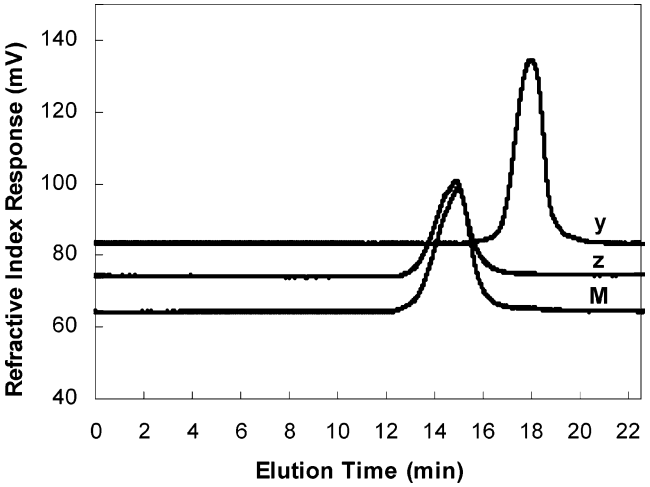

Figure 2. GPC chromatographs of **M**, **y**, and **z**. The absence of **y** (and hence **z**) confirms that **M** is the product of the monosubstituted **3** and **CH₂═CH−PDMS-*n*-Bu**.

Rh-catalyzed hydrosilylation reaction was regioselective, then the product would be pure, monosubstituted **3** (M_n = 1286 g/mol), which would subsequently react with **CH₂═CH−PDMS-*n*-Bu** to form a single product **(x)** (M_n = 61 286 g/mol). However, non-regioselective Rh-catalyzed hydrosilylation would have produced a mixture of **i**−**iii**, which would each subsequently react with **CH₂═CH−PDMS-*n*-Bu** to yield, **x**, the product of monosubstituted **3** + **CH₂═CH−PDMS-*n*-Bu** (M_n = 61 286 g/mol), **y**, unreacted α,ω-triethoxysilylethyl-disubstituted product (M_n = 1476 g/mol), and **z**, the product of **ODMS₁₃** + **CH₂═CH−PDMS-*n*-Bu** (1:2 molar ratio) ($M_n \approx$ 121 096 g/mol), where **y** and **z** would be present in equal amounts (Figure S2 of the Supporting Information). Products **y** and **z** were individually synthesized in isolated reactions so that their elution peaks could be identified in the GPC chromatograph of **M** if present. Product **y** was synthesized by Pt-catalyzed hydrosilylation of **ODMS₁₃** and **VTEOS** (1:2 molar ratio), whereas **z** was prepared by Pt-catalyzed hydrosilylation of **ODMS₁₃** and **CH₂═CH−PDMS-*n*-Bu** (1:2 molar ratio). In the GPC chromatograph of **M**, the elution peak of **y** is definitively absent (Figure 2). The elution peak of **z** would overlap with the elution peak of **M** but must be absent as well since **y** and **z** would be present in equal amounts. Thus, the composition of **M** may be identified as that of **x** (i.e., the product of monosubstituted **3** + **CH₂═CH−PDMS-*n*-Bu**). These results confirm that Rh-catalyzed hydrosilylation of reaction of **ODMS₁₃** and **VTEOS** was regioselective and produced only monosubstituted **3**. It is assumed that, because of their lower MWs, α,ω-bis(Si−H)oligodimethylsiloxanes **ODMS₀** and **ODMS₄** similarly underwent regioselective hydrosilylation to produce only monosubstituted **1** and **2**, respectively.

The monosubstituted structure of **1**−**3** is also supported by results of the measured amount of un-cross-linked material in cured films (Table 1). If Rh-catalyzed hydrosilylation was non-regioselective and produced the mixture of products **(i**−**iii)**, then **ii** (disubstituted) and **iii** (nonsubstituted) would be present in equal amounts (Figure S2 of the Supporting Information). Although **ii** would undergo sol−gel cross-linking with **P**, **iii** could not undergo cross-linking and thus would be removed as un-cross-linked material. For films prepared with a stoichiometric balance of $(EtO)_3Si-$ **(a**−**c)** and Si−OH **(P)** (i.e., films **a_2P_3, b_2P_3,** and **c_2P_3**), ≤1 wt % of un-cross-linked material was extracted. Thus, **ii** and **iii** are not present at greater than 1 wt % each. These results indicate that **1**−**3** are ≥98% monosubstituted.

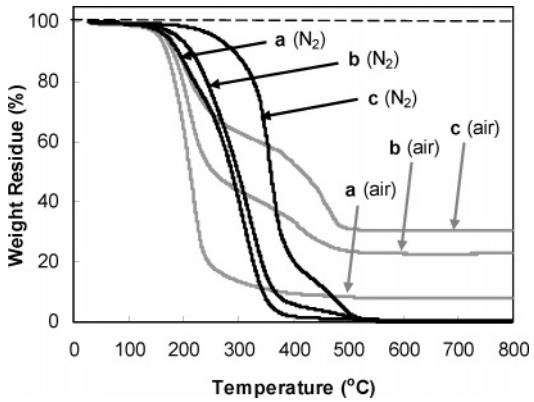

Figure 3. Thermal stability of **a**−**c** in N_2 and in air.

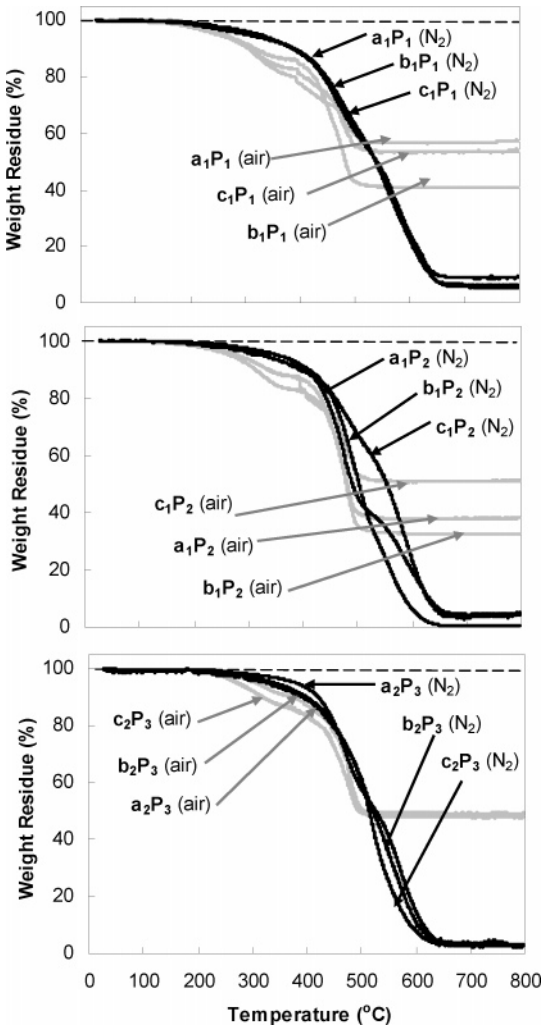

Figure 4. Thermal stability of films in N_2 and in air.

Synthesis of a−**c.** The Pt-catalyzed hydrosilyation reaction of a 1:1 molar ratio of **1**−**3** each with **A-PEO₈M** produced **a**−**c,** respectively, in good yields (≥88%). Completion of the reaction was confirmed by IR analysis of **a**−**c**, which showed no absorbance at ∼2125 cm^{-1} due to unreacted Si−H bonds of **1**−**3**, respectively. The Si−H peak (∼4.7 ppm) of ^1H NMR spectra of **a**−**c** was also absent. No vinyl peaks were observed in the ^1H or ^{13}C NMR spectra.

Thermal Stability of a−**c.** As expected, **a**−**c** began to degrade at lower temperatures in air than in N_2 (Figure 3). Polysiloxanes are known to display exceptional thermal stability compared to many organic polymers.[50] Thus, thermal stability

Table 2. Mechanical and Surface Properties of Films

	DMA	static contact angles		dynamic contact angles	
film	T_g (°C)	θ_{static} (deg) (at 15 s)	θ_{static} (deg) (at 2 min)	θ_{adv} (deg)	θ_{rec} (deg)
a_1P_1	−117	93 ± 2	77 ± 3	93 ± 1	85 ± 1
b_1P_1	−116	87 ± 2	71 ± 2	87 ± 1	78 ± 1
c_1P_1	−116	78 ± 1	64 ± 1	89 ± 1	78 ± 1
a_1P_2	−116	96 ± 1	71 ± 1	97 ± 1	81 ± 2
b_1P_2	−116	90 ± 1	62 ± 1	89 ± 1	77 ± 1
c_1P_2	−117	94 ± 1	66 ± 1	94 ± 1	77 ± 2
a_2P_3	−115	97 ± 2	78 ± 1	102 ± 1	86 ± 1
b_2P_3	−114	89 ± 1	63 ± 2	84 ± 1	70 ± 1
c_2P_3	−114	74 ± 2	61 ± 2	81 ± 1	70 ± 1
PDMS[a]		116 ± 1	115 ± 1	121 ± 1	115 ± 1
PEO[b]		62 ± 6	53 ± 4	61 ± 1	61 ± 1

[a] **PDMS** (control) = Silastic T-2 (silicone elastomer) cured on a glass microscope slide. [b] **PEO** (control) = $(EtO)_3Si-(CH_2)_3-(OCH_2CH_2)_8-OCH_3$ grafted onto a glass microscope slide.

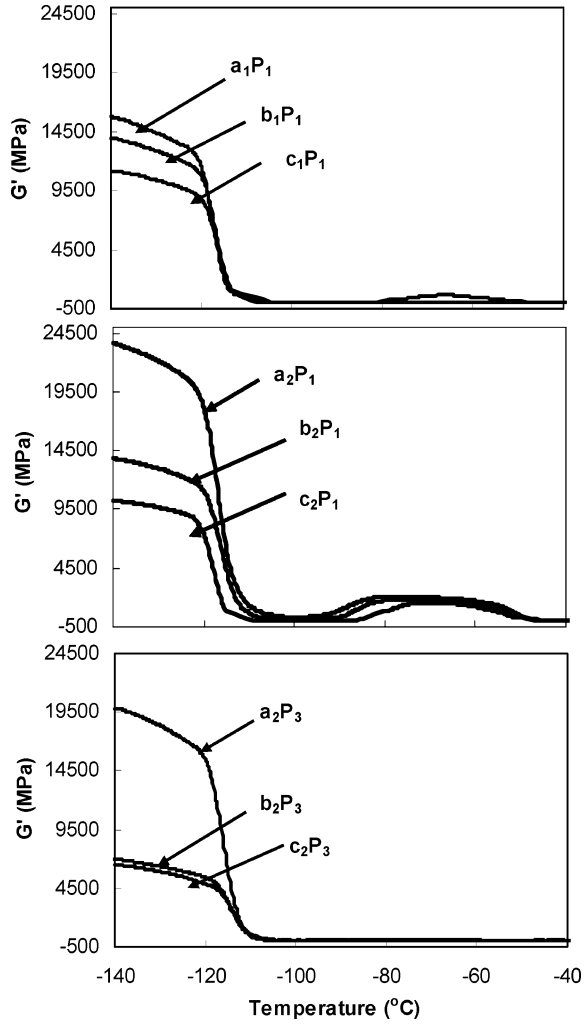

Figure 5. Storage moduli (G') of films.

in N_2 and air increased with the increasing length of the siloxane tether such that **c** was the most stable. Degradation of polysiloxanes in air produces silica residue.[50] Thus, the residue weight was highest for **c** (~30%) because of its relatively higher siloxane content.

Preparation of Films. The H_3PO_4-catalyzed sol−gel cross-linking of **a**−**c** each with **P** in varying molar ratios (1:1, 1:2, and 2:3 molar ratios of **a**, **b**, or **c** to **P**) produced a series of nine films (Figure 1 and Table 1). Commonly used tin-based

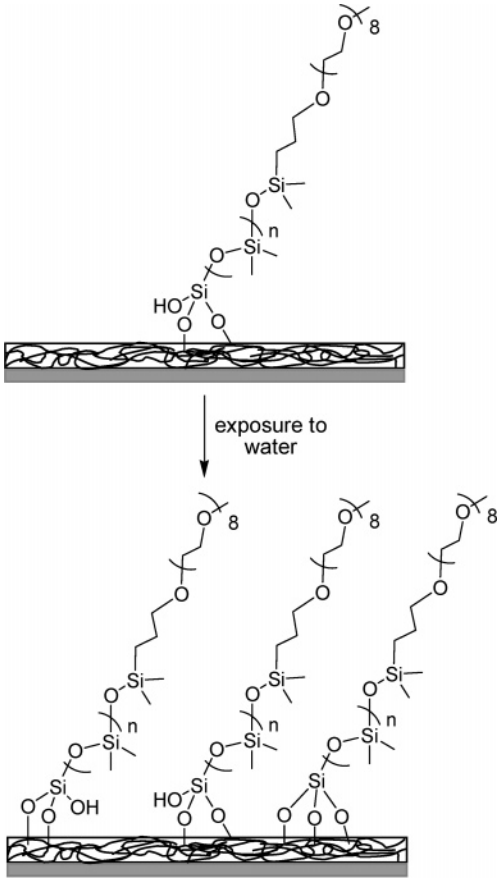

Figure 6. Following exposure to an aqueous environment, the PEO segments of **a**−**c** reorganized to the film−water interface thereby increasing surface hydrophilicity. Surface hydrophilicity increased as the siloxane tether length of **a**−**c** increased. Thus, longer siloxane tethers enhance reorganization of PEO segments to the surface.

catalysts (e.g., dibutyltin dilaurate) often require long cure schedules, and residues may have adverse effects in medical applications.[51−53] H_3PO_4 is an attractive water-soluble catalyst alternative as it may be extracted from the final product. The rate of H_3PO_4-catalyzed sol−gel condensation involving Si(OEt)$_4$ was increased by nearly 2 orders compared to other acids.[54] Gädda et al. reported the H_3PO_4-catalyzed cross-linking of α,ω-bis(Si−OH)polydimethylsiloxane and tetrakis(hydroxyldimethylsiloxane)silane.[47]

The extent of cross-linking was evaluated by Soxhlet extraction. Because there are three EtO− groups (**a**−**c**) versus two HO−Si groups (**P**) per respective chain, a 2:3 molar ratio of **a**, **b**, or **c** to **P** is stoichiometrically balanced. Thus, for films **a_2P_3**, **b_2P_3**, and **c_2P_3**, ≤1 wt % of un-cross-linked material was removed following Soxhlet extraction (Table 1). Films prepared with a stoichiometric deficiency of **P** (films **a_1P_1**, **b_1P_1**, and **c_1P_1**) or a stoichiometric excess of **P** (**a_1P_2**, **b_1P_2**, and **c_1P_2**) demonstrated greater weight loss following Soxhlet extraction (1−9 wt %).

The deconvoluted C 1s X-ray photoelectron spectrum of the surface of the $(EtO)_3Si-(CH_2)_3-(OCH_2CH_2)_8-OCH_3$-grafted microscope slide revealed three peaks: 285.0 eV (C−C), 286.7 eV (C−O), and 288.7 eV (adsorbed CO_2) (Figure S1 of the Supporting Information). The peak at 286.7 eV is consistent with the ether carbons of PEO.[55]

Thermal Stability of Films. The thermal degradation of films is shown in Figure 4. Films exhibited generally similar degradation profiles. In N_2, films were degraded by ~650 °C, whereas in air films reached their final weight by ~500 °C. In air, ~30−

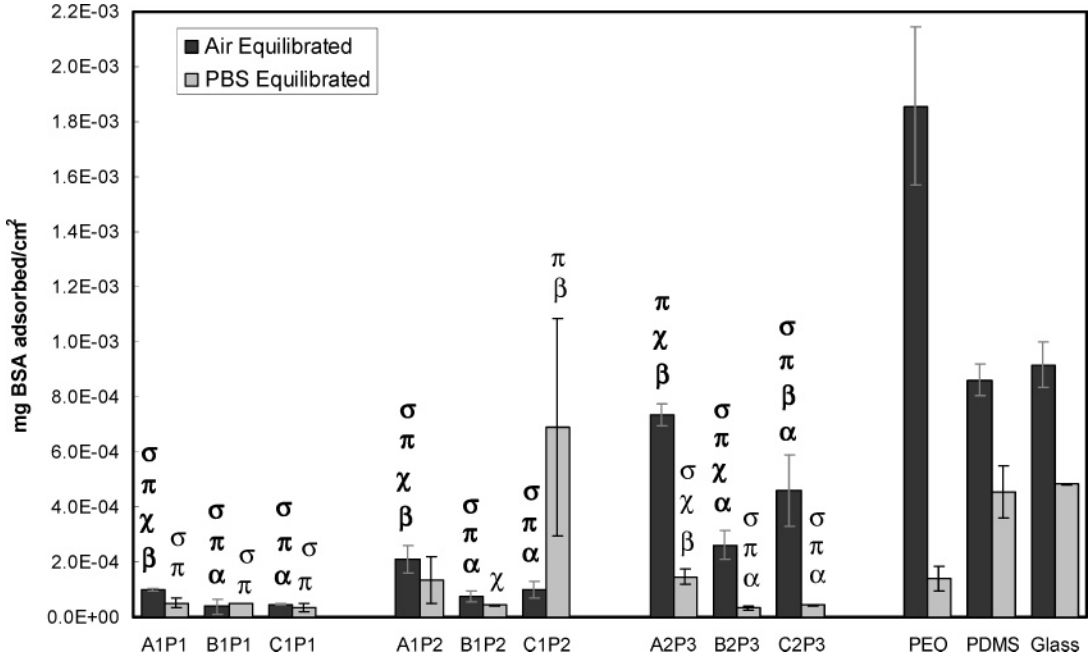

Figure 7. Adsorption of BSA protein (3 h) after film surfaces were exposed to air (air-equilibrated) and after first equilibrating in PBS for 12 h (PBS-equilibrated). Error bars represent the standard deviation between the fluorescence measurements of three randomly selected regions. For a set of films prepared at the same molar ratio (i.e., 1:1, 1:2, or 2:3 of **a**, **b**, or **c** to **P**) and with same type of exposure before BSA adsorption (e.g., air- or PBS-equilibrated), statistical significance was determined by one-way analysis of variance (Holm−Sidak method; $p = 0.05$). Symbol key: α = different than film prepared with **a**; β = different than film prepared with **b**; χ = different than film prepared with **c**; π = different than PEO control; σ = different than PDMS control.

50% of silica residue was produced for all films and is within the expected range. A slight increase in thermal stability is indicated for films $\mathbf{a_2P_3}$, $\mathbf{b_2P_3}$, and $\mathbf{c_2P_3}$, which have the least amount of un-cross-linked material. Acids are known to catalyze chain equilibration of siloxane (Si−O) bonds into low-MW cyclics, which are volatile at elevated temperatures.[50] However, the high thermal stabilities and residue weights (in air) of the films indicate that the presence of catalytic amounts of H_3PO_4 do not contribute to a reduction in their thermal stability.

Dynamic Mechanical Analysis. The mechanical properties of the films determined by DMA are summarized in Table 2. The T_g of each film was determined by the maximum of the loss modulus (G'').[56] The T_g's were low for all films and ranged between −117 and −114 °C. Similar T_g values were expected since the distance between cross-links is maintained at a constant value by the MW of **P**.[57] The presence of small amounts of un-cross-linked **a**−**c** (films $\mathbf{a_1P_1}$, $\mathbf{b_1P_1}$, and $\mathbf{c_1P_1}$) or **P** (films $\mathbf{a_1P_2}$, $\mathbf{b_1P_2}$, and $\mathbf{c_1P_2}$) did not significantly alter T_g values. Following cross-linking, the PEO segment of **a**−**c** exists as a "dangling free end". However, due to the low cross-link density of the films, the β transition temperature (T_β) associated with such free ends is not observed nor is a decrease in T_g with increased siloxane tether length.[58] Lower-MW analogues of **P** may be utilized to prepare more densely cross-linked films with higher T_g's, which may reveal the aforementioned trends.

The storage modulus (G') is related to stiffness or resistance to deformation.[59] For films prepared with the same molar ratio of **a**, **b**, or **c** to **P**, G' increased with decreasing siloxane tether length in the order **c** < **b** < **a** (Figure 5).

Contact Angle Analysis. Contact angle measurements of water droplets on film surfaces are reported in Table 2. The hydrophobic PDMS control produced a high θ_{static} (at 15 s) (116°) whereas θ_{static} (at 15 s) of the hydrophilic PEO control was low (62°). For films prepared with the same molar ratio (**a**−**c** to **P**), θ_{static} (at 15 s) decreased and surface hydrophilicity increased in the order **a** < **b** < **c**. Furthermore, θ_{static} (at 2 min) was significantly lower than the corresponding θ_{static} (at 15 s), and hydrophilicity similarly increased in the order **a** < **b** < **c**. The exception to this trend was noted for film $\mathbf{c_1P_2}$, which displayed slightly higher θ_{static} values compared to $\mathbf{b_1P_2}$. Un-cross-linked material may have migrated to the film surface and altered surface properties. Films prepared with a 2:3 molar ratio (**a**−**c** to **P**) lack significant quantities of un-cross-linked material that may have migrated to the film surface. For these films, increased siloxane tether length **(a**−**c)** produced surfaces with enhanced hydrophilicity. Thus, longer siloxane tethers more effectively mobilized PEO segments to the surface (Figure 6).

The hydrophobic surface characteristics are obtained from θ_{adv} whereas hydrophilicity is reflected by θ_{rec}.[60] For cross-linked silicones, the presence of Si−CH_3 groups at the film−air interface leads to high θ_{adv}. After a pure silicone surface is wetted, polar groups such as Si−O−Si reorganize to the film−water interface to minimize interfacial tension such that $\theta_{rec} < \theta_{adv}$.[61] For all films, θ_{rec} was significantly reduced versus the corresponding θ_{adv}, indicating that PEO reorganized to the surface after exposure to water.[62] As previously mentioned, surface compositions of films prepared with a 2:3 molar ratio (**a**−**c** to **P**) are not potentially complicated by the presence of un-cross-linked materials at the surface. For these films, increased siloxane tether length **(a**−**c)** enhanced hydrophilicity before and after exposure to an aqueous environment (i.e., lower θ_{adv} and θ_{rec}) in the order of **a** < **b** < **c**. These observations support the conclusion that longer siloxane tethers more effectively mobilize PEO to the surface particularly when exposed to aqueous environments (Figure 6).

Protein Adsorption. The adsorption of BSA protein onto film surfaces and controls are reported in Figure 7. For a given set of films prepared with the same molar ratio (**a**−**c** to **P**), statistical differences ($p < 0.05$) are noted within that series and compared to the PDMS and PEO controls. BSA adsorption onto the PEO control (air-equilibrated) was unusually high possibly due to insufficient PEO hydration produced by the

experimental protocol.[26] It was observed that films (air-equilibrated) generally adsorbed less BSA compared to the PDMS control (air-equilibrated). Films exhibited enhanced surface hydrophilicity compared to the PDMS control as was indicated by their lower θ_{adv} values (Table 2). Thus, PEO is present at film surfaces prior to exposure to an aqueous environment, which leads to reduced protein adsorption. There was not a statistical difference in the amount of BSA adsorbed onto film $\mathbf{a_2P_3}$ (air-equilibrated) compared to the PDMS control. Its relatively high BSA adsorption may be attributed to the fact that this film was the most hydrophobic ($\theta_{adv} = 102°$).

For films prepared with 1:1 and 2:3 molar ratio (**a**−**c** to **P**), equilibration in PBS for 12 h just prior to exposure to BSA (PBS-equilibrated) significantly reduced BSA adsorption compared to the PDMS control (PBS-equilibrated) as well as the PEO control (PBS-equilibrated). These films exhibited lower θ_{static} (2 min) and θ_{rec} values compared to the PDMS control. Also, these values are much lower than the corresponding θ_{static} (15 s) and θ_{adv}, which indicates that additional PEO mobilized to the surface upon exposure to an aqueous environment (Figure 6). The enhancement of PEO to the surface improves protein repellency. Adsorption of BSA onto film $\mathbf{a_2P_3}$ (PBS-equilibrated) versus the PEO control (PBS-equilibrated) was not statistically different. It was the least hydrophilic of all films ($\theta_{rec} = 86°$).

Films prepared with a stoichiometric excess of **P** (1:2 molar ratio of **a**−**c** to **P**; PBS-equilibrated) demonstrated different BSA adsorption results. Film $\mathbf{c_1P_2}$ showed higher BSA adsorption after equilibration in PBS; this result was repeated in a second analysis. Also, films $\mathbf{a_1P_2}$ and $\mathbf{b_1P_2}$ (PBS-equilibrated) did not adsorb statistically different amounts of BSA compared to the PDMS and PEO controls (PBS-equilibrated). The presence of un-cross-linked **P** at these film surfaces may have contributed to these results.

The effect of siloxane tether **(a**−**c)** length on protein resistance may be evaluated with films prepared with a 2:3 molar ratio (**a**−**c** to **P**). Films $\mathbf{b_2P_3}$ and $\mathbf{c_2P_3}$ (PBS-equilibrated) adsorbed less BSA compared to film $\mathbf{a_2P_3}$ (PBS-equilibrated) as well as the PDMS and PEO controls. The amount of BSA adsorbed onto $\mathbf{b_2P_3}$ versus $\mathbf{c_2P_3}$ (PBS-equilibrated) was not statistically different. Thus, increased siloxane tether length enhanced mobilization of PEO to the surface following exposure to an aqueous environment leading to improved protein resistance.

Conclusions

PEO chains were incorporated into silicones via siloxane tethers **(a**−**c)** of varying lengths to systematically increase PEO mobilization to the film surface and improve protein resistance. Three unique ambifunctional molecules **(a**−**c)** having the general formula α-$(EtO)_3Si(CH_2)_2$−oligodimethylsiloxane$_n$-*block*-poly(ethylene oxide)$_8$−OCH_3 ($n = 0$ **(a)**, 4, **(b)**, and 13 **(c)**) were prepared via regioselective Rh-catalyzed hydrosilylation. H_3PO_4-catalyzed sol−gel cross-linking of **a**−**c** each with α,ω-bis(Si−OH)polydimethylsiloxane (**P**, $M_n = 3000$ g/mol) in varying ratios (1:1, 1:2, and 2:3 molar ratios of **a**, **b**, or **c** to **P**) produced nine films. These films exhibited very low T_g and G' values as well as high thermal stability. The effects of the siloxane tether length **(a**−**c)** on surface properties and protein resistance were readily assessed with films prepared with a 2:3 molar ratio (**a**−**c** to **P**) that are not complicated by the presence of un-cross-linked materials that may migrate to the film surface. For these films, increased length of the siloxane tether **(a**−**c)** produced surfaces with increased hydrophilicity, which was further enhanced upon exposure to an aqueous environment. Less BSA protein was adsorbed onto films $\mathbf{b_2P_3}$ and $\mathbf{c_2P_3}$ (PBS-equilibrated) compared to film $\mathbf{a_2P_3}$ (PBS-equilibrated) as well compared to the PDMS and PEO controls. Films $\mathbf{b_2P_3}$ and $\mathbf{c_2P_3}$ (PBS-equilibrated) adsorbed statistically similar amounts of BSA. Thus, the increased siloxane tether length of **a**−**c** enhanced protein resistance of silicone-based films by more effectively mobilizing PEO to the surface particularly after exposure to an aqueous environment.

Acknowledgment. The authors thank D. E. Bergbreiter (Department of Chemistry, Texas A&M University) for use of the CAM-200 contact angle analyzer.

Supporting Information Available. XPS scan of $(EtO)_3Si(CH_2)_3(OCH_2CH_2)_8OCH_3$ chemically grafted onto a glass microscope slide, schematic of the preparation of **i**−**iii** and **x**−**z**, and preparation of **y** and **z** for GPC studies. This material is available free of charge via the Internet at http://pubs.acs.org.

References and Notes

(1) Dyke, M. E. V.; Clarson, S. J.; Arshady, R. Silicone biomaterials. In *Introduction to Polymeric Biomaterials*; Arshady, R., Ed.; Citus Books: London, 2003; Vol. 1, pp 109−135.
(2) Curtis, J.; Colas, A. Medical applications of silicones. In *Biomaterials Science*, 2nd ed.; Ratner, B. D., Hoffman, A. S., Schoen, F. J., Lemons, J. E., Eds.; Elsevier Academic Press: San Diego, CA, 2004; pp 697−707.
(3) Hron, P. *Polym. Int.* **2003**, *52*, 1531−1539.
(4) Bartzoka, V.; McDermott, M. R.; Brook, M. A. *Adv. Mater.* **1999**, *11*, 257−259.
(5) Pitt, W. G.; Park, K.; Cooper, S. L. *J. Colloid Interface Sci.* **1986**, *111*, 343−362.
(6) Sharma, C. P. *J. Biomater. Appl.* **2001**, *15*, 359−381.
(7) Bodas, D.; Khan-Malek, C. *Microelectron. Eng.* **2006**, *83*, 1277−1279.
(8) Zhang, H.; Annich, G. M.; Miskulin, J.; Osterholzer, K.; Merz, S. I.; Bartlett, R. H.; Meyerhoff, M. E. *Biomaterials* **2002**, *23*, 1485−1494.
(9) Yao, K.; Huang, X.-D.; Huang, X.-J.; Xu, Z.-K. *J. Biomed. Mater. Res., Part A* **2006**, *78*, 684−692.
(10) Abbasi, F.; Mirzadeh, H.; Katbab, A.-A. *Polym. Int.* **2001**, *50*, 1279−1287.
(11) Gombotz, W. R.; Guanghui, W.; Horbett, T. A.; Hoffman, A. S. *J. Biomed. Mater. Res.* **1991**, *25*, 1547−1562.
(12) Lee, J. H.; Lee, H. B.; Andrade, J. D. *Prog. Polym. Sci.* **1995**, *20*, 1043−1079.
(13) Owen, M. J.; Smith, P. J. *J. Adhes. Sci. Technol.* **1994**, *8*, 1063−1075.
(14) Kuznetsov, A. Y.; Bagryansky, V. A.; Perov, A. K. *J. Appl. Polym. Sci.* **1995**, *57*, 201−207.
(15) Xia, Y.; Whitesides, G. M. *Angew. Chem., Int. Ed.* **1998**, *37*, 550−575.
(16) Efimenko, K.; Wallace, W. E.; Genzer, J. *J. Colloid Interface Sci.* **2002**, *254*, 306−315.
(17) Graubner, V.-M.; Jordan, R.; Nuyken, O.; Schnyder, B.; Lippert, T.; Kotz, R.; Wokaun, A. *Macromolecules* **2004**, *37*, 5936−5943.
(18) Efimenko, K.; Crowe, J. A.; Manias, E.; Schwark, D. W.; Fischer, D. A.; Genzer, J. *Polymer* **2005**, *46*, 9329−9341.
(19) Sui, G.; Wang, J.; Lee, C.-C.; Lu, W.; Lee, S. P.; Leyton, J. V.; Wu, A. M.; Tseng, H.-R. *Anal. Chem.* **2006**, *78*, 5543−5551.
(20) Brook, M. A. *Silicon in Organic, Organometallic, and Polymer Chemistry*; John Wiley & Sons: New York, 2000; pp 324−331.
(21) Papra, A.; Bernard, A.; Juncker, D.; Larsen, N. B.; Michel, B.; Delamarche, E. *Langmuir* **2001**, *17*, 4090−4095.
(22) Delamarche, E.; Donzel, C.; Kamounah, F. S.; Wolf, H.; Geissler, M.; Stutz, R.; Schmidt-Winkel, P.; Michel, B.; Mathieu, H. J.; Schaumburg, K. *Langmuir* **2003**, *19*, 8749−8758.
(23) Chen, H.; Zhang, Z.; Chen, Y.; Brook, M. A.; Sheardown, H. *Biomaterials* **2005**, *26*, 2391−2399.
(24) Chen, H.; Brook, M. A.; Sheardown, H. *Biomaterials* **2004**, *25*, 2273−2282.
(25) Chen, H.; Brook, M. A.; Chen, Y.; Sheardown, H. *J. Biomater. Sci., Polym. Ed.* **2005**, *16*, 531−548.

(26) Elbert, D. L.; Hubbel, J. A. *Annu. Rev. Mater. Sci.* **1996**, *26*, 365−394.
(27) Knoll, D.; Hermans, J. *J. Biol. Chem.* **1983**, *258*, 5710−5715.
(28) Jeon, S. I.; Lee, J. H.; Andrade, J. D.; DeGennes, P. G. *J. Colloid Interface Sci.* **1991**, *142*, 149−158.
(29) Jeon, S. I.; Andrade, J. D. *J. Colloid Interface Sci.* **1991**, *142*, 159−166.
(30) McPherson, T.; Kidane, A.; Szleifer, I.; Park, K. *Langmuir* **1998**, *14*, 176−186.
(31) Osterberg, E.; Bergstrom, K.; Holmberg, K.; Riggs, J. A.; Alstine, J. M. V.; Schuman, T. P.; Burns, N. L.; Harris, J. M. *Colloids Surf., A* **1993**, *77*, 159−169.
(32) Desai, N. P.; Hubbel, J. A. *Biomaterials* **1991**, *12*, 144−153.
(33) Berstrom, K.; Holmber, K.; Safranj, A.; Hoffman, A. S.; Edgell, M. J.; Kozlowski, A.; Hovanes, B. A.; Harris, J. M. *J. Biomed. Mater. Res.* **1992**, *26*, 779−790.
(34) Desai, N. P.; Hubbell, J. A. *J. Biomed. Mater. Res.* **1991**, *25*, 829−843.
(35) Prime, K. L.; Whitesides, G. M. *Science* **1991**, *252*, 1164−1166.
(36) Prime, K. L.; Whitesides, G. M. *J. Am. Chem. Soc.* **1993**, *115*, 10714−10721.
(37) Sofia, S. J.; Premnath, V.; Merrill, E. W. *Macromolecules* **1998**, *31*, 5059−5070.
(38) Mark, J. E. Silicon-containing polymers. In *Silicon-Based Polymer Science: A Comprehensive Resource*; Zeigler, J. M., Fearon, F. W. G., Eds.; Advances in Chemistry Series 224; American Chemical Society: Washington, DC, 1990; pp 47−53.
(39) Lane, T. H.; Burns, S. A. Silica, silicon, and silicones... Unraveling the mystery. In *Immunology of Silicones*; Potter, M., Rose, N. R., Eds.; Springer: Berlin, 1996; p 7.
(40) Crivello, J. V.; Bi, D. *J. Polym. Sci., Part A: Polym. Chem.* **1993**, *31*, 2563−2572.
(41) Crivello, J. V.; Bi, D. *J. Polym., Sci. Part A: Polym. Chem.* **1993**, *31*, 2729−2737.
(42) Crivello, J. V.; Bi, D. *J. Polym. Sci., Part A: Polym. Chem.* **1993**, *31*, 3109−3119.
(43) Crivello, J. V.; Bi, D. *J. Polym. Sci., Part A: Polym. Chem.* **1993**, *31*, 3121−3132.
(44) Grubb, W. T.; Osthoff, R. O. *J. Am. Chem. Soc.* **1954**, *76*, 5190−5197.
(45) Mabry, J. M.; Paulasaari, J. K.; Weber, W. P. *Polymer* **2000**, *41*, 4423−4428.
(46) Hooper, R.; Lyons, L. J.; Mapes, M. K.; Schumacher, D. *Macromolecules* **2001**, *34*, 931−936.
(47) Gädda, T. M.; Kus, E.; Mansfeld, F.; Finlay, J. A.; Callow, J. A.; Callow, M. E.; Kowalke, G. L.; Wendt, D. E.; Weber, W. P. *J. Polym. Sci., Part A: Polym. Chem.* **2006**, *44*, 2237−2247.
(48) Gudipati, C. S.; Finlay, J. A.; Callow, J. A.; Callow, M. E.; Wooley, K. L. *Langmuir* **2005**, *21*, 3044−3053.
(49) Nagashima, H.; Tatebe, K.; Ishibashi, T.; Sakaklbara, J.; Itoh, K. *Organometallics* **1989**, *8*, 2495−2496.
(50) Dvornic, P. R. Thermal properties of polysiloxanes. In *Silicon-Containing Polymers: The Science and Technology of Their Synthesis and Applications*; Jones, R. G., Ando, W., Chojnowski, J., Eds.; Kluwer Academic Publishers: Dordrecht, The Netherlands, 2000; pp 200−210.
(51) Johnston, E.; Bullock, S.; Uilk, J.; Gatenholm, P.; Wynne, K. J. *Macromolecules* **1999**, *32*, 8173−8182.
(52) Uilk, J.; Bullock, S.; Johnston, E.; Meyers, S. A.; Merwin, L.; Wynne, K. J. *Macromolecules* **2000**, *33*, 8791−8801.
(53) Alam, M. S.; Husain, R.; Seth, P. K.; Srivastava, S. P. *Bull. Environ. Contam. Toxicol.* **1993**, *50*, 286−292.
(54) Cihlar, J. *Colloids. Surf., A* **1993**, *70*, 253−268.
(55) Moreau, O.; Portella, C.; Massicot, F.; Herry, J. M.; Riquet, A. M. *Surf. Coat. Technol.* **2007**, *201*, 5994−6004.
(56) Sperling, L. H. In *Introduction to Physical Polymer Science*, 3rd ed.; John Wiley & Sons: New York, 2001; p 308.
(57) Sperling, L. H. In *Introduction to Physical Polymer Science*, 3rd ed.; John Wiley & Sons: New York, 2001; p 335.
(58) Menard, K. P. In *Dynamic Mechanical Analysis: A Practical Introduction*; CRC Press: Boca Raton, FL, 1999; p 95.
(59) Wicks, Z. W., Jr.; Jones, F. N.; Pappas, S. P. *Organic Coatings Science and Technology*, 2nd ed.; John Wiley & Sons: New York, 1999; pp 68−69.
(60) Davies, J.; Nunnerley, C. S.; Brisley, A. C.; Edwards, J. C.; Finalyson, S. D. *J. Colloid Interface Sci.* **1996**, *182*, 437−443.
(61) Owen, M. J. Siloxane surface activity. In *Silicon-Based Polymer Science: A Comprehensive Resource*; Zeigler, J. M., Fearon, F. W. G., Eds.; Advances in Chemistry Series 224; American Chemical Society: Washington, DC, 1990; pp 705−739.
(62) Johnson, R. E., Jr.; Dettre, R. H. *J. Phys. Chem.* **1964**, *68*, 1744−1750.

BM700543C